A variational approach to design a numerical scheme on an arbitrary moving grid for N-fluid flow with thermodynamic consistency

T. VAZQUEZ-GONZALEZ[a], A. LLOR[b], C. FOCHESATO[c]

a. CEA, DAM, DIF, 91297 Arpajon Cedex, France, thibaud.vazquez-gonzalez@cea.fr
b. CEA, DAM, DIF, 91297 Arpajon Cedex, France, antoine.llor@cea.fr
c. CEA, DEN, DTN/SMTA/LPMA, F-13108 Saint-Paul-lez-Durance Cedex, France, christophe.fochesato@cea.fr

Abstract :

In some highly demanding fluid dynamics simulations, as for instance in inertial confinement fusion applications, it appears necessary to simulate multi-fluid flows involving numerous constraints at the same time, such as (and non-limitatively) : large numbers of fluids (typically 10 and above), both isentropic and strongly shocked compressible evolution, large heat sources, large deformations, transport over large distances, and highly variable or contrasted EOS stiffnesses.
Fulfilling such a challenge in a robust and tractable way demands that thermodynamic consistency of the numerical scheme be carefully ensured. This is addressed here over an arbitrarily evolving computational grid (ALE or Arbitrary Lagrangian–Eulerian approach) by a three-step mimicking derivation using a GEEC (Geometry, Energy, and Entropy Compatible) procedure (see [2] for details) : i) to ensure a compatible (approximately symplectic) exchange between internal and kinetic energies under isentropic conditions, a variational least action principle is used to generate the proper pressure forces in the momentum equations ; ii) to generate the conservative internal energy equation, a tally is performed to match the kinetic energy, and iii) artificial dissipation is added to ensure shock stability, but other physical terms could also be included (drag, heat exchange, etc.).
Varied single-, two- and multi-fluid test cases show satisfactory behavior, including the 2D, close-to-sonic, high volume-fraction convergence of eight Gaussian packets of different stiffened-gas fluids in a background of perfect gas (under the sole pressure coupling).

Mots clefs : Direct-ALE, compressible fluid, multiphase flows, shocks

1 Introduction

Despite intensive research over the last five decades stimulated by wide-ranging academic and industrial applications, the development of numerical schemes for the simulation of multi-phase flows remains a very active field. Numerous and recurring issues remain open or merely addressed for specific flow types—depending on nature, strength, boundaries, sources, etc. Aside of the usual

conservation laws (masses, momentum, and energy) fully general principles are few and sometimes controversial : most emblematic is the forty years old dispute about the elliptic behavior of the "backbone" dissipation-free model which has haunted most works to date [1, and references therein].
However, there appears that thermodynamic consistency—i.e. compliance with the second law of thermodynamics which forbids entropy reduction in a closed system—is seldom given the attention it deserves in numerical schemes and could usefully complement the existing principles. It is generally assumed, most often implicitly, that if a given physical model is thermodynamically consistent, so will be its discretization up to some hopefully negligible numerical residue. In practice, this appears quite acceptable for most of the "reasonable" single fluid schemes, and possible residual inconsistencies are further expected to become insignificant by increasing numerical order. For multiphase schemes however, a much less optimistic stance must be taken as was shown recently in a review of Ransom test results from the literature [1] : it appears that *six*-equation two-phase schemes—i.e. which integrate the energy equations—can often fare much worse than *four*-equation models—which force thermodynamic consistency through an isentropic EOS closure of internal energies. This could be attributed to "hidden" entropy residues of uncontroled sign.
The present work summarizes the main features and results in the design of a new multiphase scheme named multiGEECS (multiphase GEEC Scheme) which complies with a stringent set of specifications : large numbers of fluids (typically 10 and above), both isentropic and strongly shocked compressible evolution, large heat sources, large deformations, transport over large distances, and highly variable or contrasted EOS stiffnesses. In view of the remarks above, it appeared early on in this development that thermodynamic consistency would become the major critical element. Energy transfers through pressure forces can be numerous in an N-phase flow—$N(2N-1)$ exchange terms between N kinetic and N internal energies—but always balance each other and *exactly* cancel all irreversible productions under isentropic evolution ; numerically however, these cancellations are only *approximate*, even when energy is conserved, and can be of low order or outright inconsistent if not carefully controled.

2 Summary of the GEEC schemes

For clarity, only summary of GEECS (single-fluid GEEC Scheme) and multiGEECS (multi-fluid GEEC Scheme) are presented here. Detailed step-by-step derivations and detailed evolution equations of these schemes can be found in [2] and [3] respectively. The two schemes are discretized using the same three-step discrete derivation : i) a variational least action principle is used to derive the momentum evolution equations—thus generating the proper pressure forces in the pressure gradient terms ; — ii) a tally is performed to match kinetic and internal energies in order to obtain the discrete evolution equations for the internal energy—thus ensuring the total energy conservation at discrete level ; —and iii) a artificial dissipation term is added to the evolution equations—as a pressure-like contribution—in order to capture shocks and to stabilize the schemes.
In the Lagrangian limit—i.e. no mass fluxes between cells—kinetic and internal energies are discretized to second-order in both space-and-time. As this work represents a proof of concept for the study of variational direct ALE scheme, both GEECS and multiGEECS capture transport in a very similar ways by a first-order upwind explicit scheme. The variational derivation leads to a non-standard downwind formulation of the pressure gradient, dual of the upwind transport operator. Both GEECS and multiGEECS involve the following features : i) full conservation of masses, momenta, and total energies at discrete level—up to round-off errors ; — ii) *direct* ALE formalism where mass, momentum,

and internal energy fluxes at moving cell boundaries are directly taken into account in the evolution equations—without separation between evolution phase and remapping procedure ; — iii) thermodynamic consistenty of the pressure work—hence entropy—even when the grid is not moving at the fluid speed ; iv) a CFL restricted evolution of the mesh that can be either arbitrarily specified at will by the user or adaptatively constrainted on the fly to the flow characteristics ; and v) generic discrete mass, momentum, and internal energy evolution equations are derived without any constraint on structure or spatial dimension—however all the tests reported in Section 3 are restricted to structured meshes of quadrangles in two-dimensions.
For multiGEECS, the pressure equilibrium is ensured through a simple and local (to the cells) procedure at the end of each time step.

3 Numerical results

The behavior of GEECS and multiGEECS is tested in two-dimensions by performing single- and multi-phase test cases from the literature—including Sod's shock tube, Sedov's cylindrical blast wave, water–air shock tube, Ransom's water faucet problem, and crossing of heavy packets in a surrounding light gas—with strenuous grid motion strategies. The results of these test cases confirm the following properties : i) exact conservation of masses, momenta, and total energies at discrete level up to round-off errors (on the capture of shock levels and shock velocities) ; ii) robust multi-material like behavior with small residual volume fractions ; iii) stable multi-phase like behavior with drifting between fluids ; and iv) versatility regarding grid motion strategies—including supersonic shearing, near-Lagrangian evolution, randomly distorted grid, and shrink-then-stretch swirling mesh.

In all the test cases, perfect gas and stiffened gas equations of state are used for the description of the fluids. The relationship between pressure, density and internal energy are given by

$$P = (\gamma - 1)\rho e \ , \qquad\qquad P = (\gamma - 1)\rho e - \pi \ . \tag{1}$$

where γ, P [Pa], ρ [kg/m^3], and e [J/kg] are the isentropic coefficient, pressure, density, and internal energy of the fluid respectively. For water, the stiffened gas constant is supposed to be close to $\pi = 21.10^8$ Pa.
The results section for both single-phase (GEECS) and multi-phase schemes (multiGEECS) is organized as follows : i) in Section 3.1, a variant of the single-phase Sod's shock tube is performed with GEECS on a sheared grid across the y direction. This sheared variant verifiy the ability of the scheme to comply with the tilting of the fluid characteristics ; ii) in Section 3.2, Sedov's cylindrical blast wave is run with GEECS with near-Lagrangian grid velocity in order to remove almost completely the numerical diffusion ; iii) in Section 3.3, the two-fluid water–air shock tube is performed with multiGEECS on a sheared grid in the y direction. An infinite drag force term is set between the fluids—the absolute velocity is averaged for each fluid at each cycle—in order to verify the ability of the scheme to handle artificial interface problem ; iv) in Section 3.4, a two-fluid Ransom's water faucet problem is run with multiGEECS on a grid randomly distorted at each cycle ; and v) in Section 3.5, a nine-fluid crossing test of eight packets of heavy fluids in a surrounding light gas is performed with multiGEECS on a shrink-then-stretch swirling ALE mesh.

3.1 2D Sod's shock tube on mesh sheared across the y direction

This classical Riemann problem for perfect gas (1)—whose initial conditions can be found in [7]—produces an expansion fan, a contact discontinuity, and a shock of medium strength. The initial domain is set to $\Omega = [0; 1] \times [-0.3; 0.6]$. Figure 1 represents a variant of Sod's shock tube where the grid velocity is given by $w_x = 5y$ and $w_y = 0$. The grid is thus sheared across the y direction with maximal and minimal values for the velocity of respectively $w_x = 3$ at $y = 0.6$ and $w_x = -1.5$ at $y = -0.3$. This variant verifies the ability of GEECS to handle large grid distortions. In particular, as the grid velocity goes from $w_x = 3$ to $w_x = -1.5$ it shifts the characteristics and the scheme must capture precisely the position of the shock and contact discontinuity—black lines shown in Figure 1(a) represent the Lagrangian and supersonic fluid velocities computed by $\pm\sqrt{\gamma P/\rho} + \mu$.

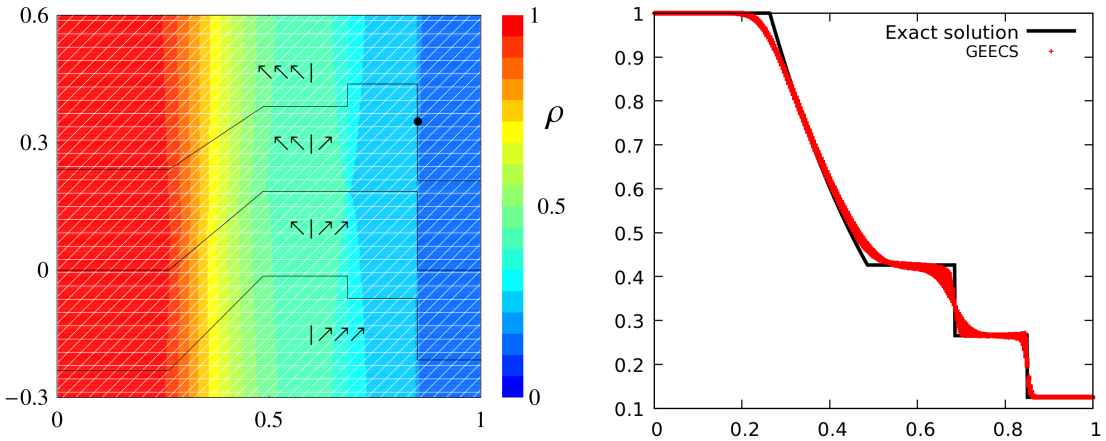

(a) Two-dimensional density map

(b) One-dimensional superposition of all points

FIGURE 1 – Density map and profile for the two-dimensional Sod's shock tube on y sheared grid. The grid velocity is $w_x = 5y$ and $w_y = 0$. Maximums of grid velocity are supersonic relative to the fluid flow. The black lines on the density profile correspond to the Lagrangian fluid velocity and supersonic limits $\pm\sqrt{\gamma P/\rho} + \mu$. The black dot represents the shock velocity. The computations are done with $I = 320 \times 290$ cells, every displayed macro cell (white lines) corresponds to 10×10 numerical cells, and CFL $= 0.8$.

3.2 2D Sedov's cylindrical blast wave test on near-Lagrangian mesh

Sedov's blast wave [6] represents an explosion in a cold perfect gas of zero-pressure (1). The initial domain is set to $\Omega = [0; 1.2] \times [0; 1.2]$. The initial conditions are characterized by $(\rho, P, \mu) = (1, 10^{-16}, 0)$ with the isentropic coefficient $\gamma = 5/3$. An initial internal energy deposition is made at the origin in the cell located at $x = y = 0$. The magnitude of the internal energy deposition can be found in [6]. This large deposition of internal energy—prescribing the pressure at the origin through the equation of state of the fluid—creates an "infinitely strong" divergent shock that propagates in the numerical domain. Figure 2 represents the density map and the superposition of all density points for a variant of Sedov's blast wave in which the grid velocity is chosen so as to reduce the numerical diffusion on the entire numerical domain, and especially in the shock area. However, following the

fluid in a Lagrangian way involves large deformations in the first cells of the mesh. In order to capture more accurately the exact solution without suffering critical mesh deformations, the grid velocity is given by

$$\boldsymbol{w}_p^{n+1/2} = \eta\ \boldsymbol{w}_p^{\mathrm{NL}}\ , \qquad \text{with} \qquad \eta = (t/t_0)^2 \,/\, \left(1 + (t/t_0)^2\right)\ , \tag{2}$$

where $\boldsymbol{w}_p^{\mathrm{NL}}$ is the near-Lagrangian grid velocity computed by the scheme, and η is a time increasing factor corresponding to the Eulerian to Lagrangian transition time. For the present two-dimensional Sedov's blast wave, the Eulerian to Lagrangian transition time was chosen to be $t_0 = 0.1$.

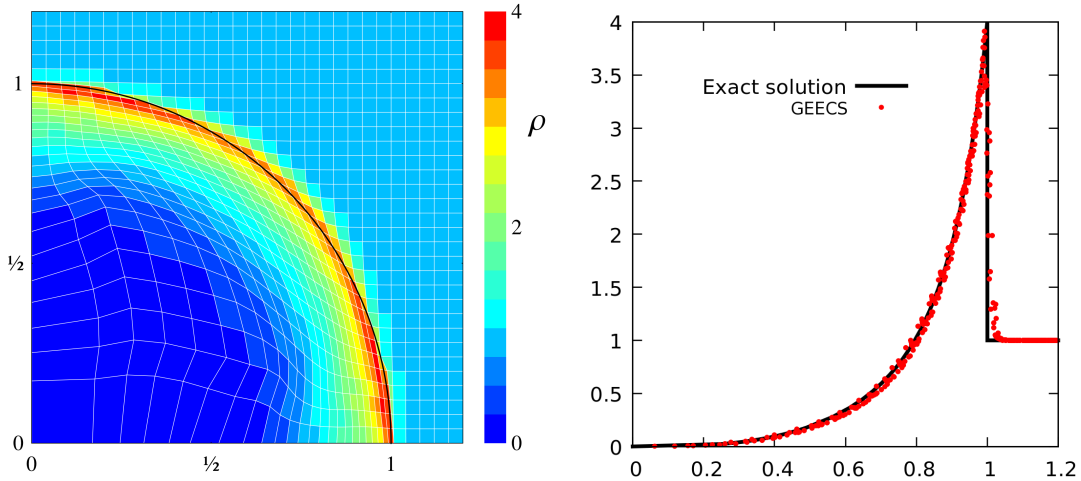

(a) Two-dimensional density map (b) One-dimensional superposition of all points

FIGURE 2 – Two-dimensional view (left) and one-dimensional superposition of all the points (right) for the ALE two-dimensional Sedov's blast wave. The grid velocity is given by (2). The computations are done with $I = 40 \times 40$ cells, every displayed macro cell (white lines) corresponds to 1×1 numerical cells, CFL $= 0.8$, and an initial numerical area $\Omega = [0; 1.2] \times [0; 1.2]$.

3.3 2D two-fluid water–air shock tube on mesh sheared across the y direction

This two-phase Riemann problem represents a more challenging test than Sod's shock tube done in Section 3.1. The initial domain is set to $\Omega = [0; 1] \times [-0.4; 0.9]$. The equations of state of water and air are approximated by stiffened and perfect gases respectively (1). The initial conditions for densities, volume fractions, velocities, and pressure are

$$\begin{array}{lcccccc} & \rho_\pm & \alpha_+ & \alpha_- & \mu_\pm & u_\pm & P \\ x < 0.7 & 1000 & 1 - 10^{-12} & 10^{-12} & 0 & 0 & 10^9 \\ x > 0.7 & 1 & 10^{-12} & 1 - 10^{-12} & 0 & 0 & 10^5 \end{array} \tag{3}$$

The grid velocity is $w_x = 4167y$ and $w_y = 0$ with maximal and minimal values of respectively $w_x = 3750$ at $y = 0.9$ and $w_x = -1667$ at $y = -0.4$. The grid thus undergoes a shearing across the y direction with a shifting of the characteristics. The number of cells in the x and y directions, 200×260, is chosen so that the initial cells are perfect squares and at final time $t = 0.00024$ they

are exact parallelograms with a $\pi/4$ angle relative to the initial mesh.

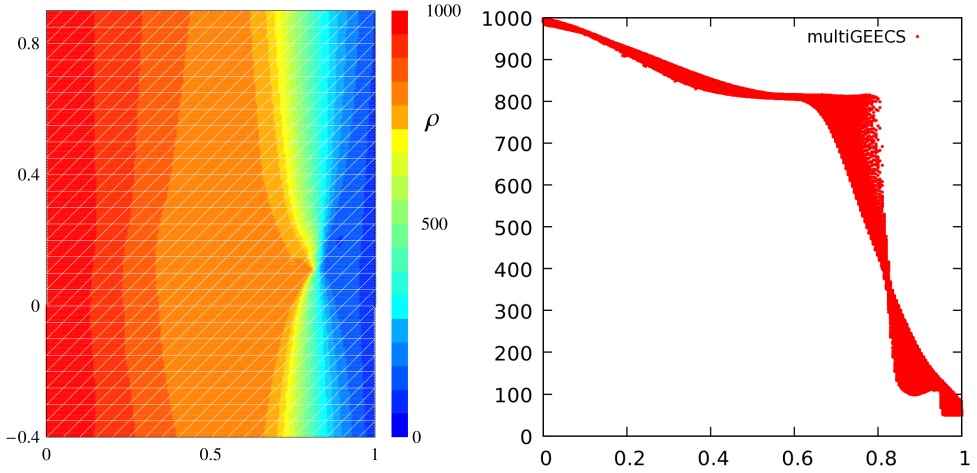

(a) Two-dimensional density map

(b) One-dimensional superposition of all density points

FIGURE 3 – Density (top) and volume fraction (bottom) maps and profiles for the two-dimensional two-fluid water–air shock tube on sheared grid across the y direction. The grid velocity is $w_x = 4167y$ and $w_y = 0$. Maximums of grid velocity are supersonic relative to the fluid flow. The computations are done with CFL $= 0.4$ and $I = 200 \times 260$ cells, every displayed macro cell (white lines corresponds to 10×10 numerical cells.

3.4 2D two-fluid Ransom water faucet problem on randomly distorted mesh

The water faucet problem of Ransom has become a basic benchmark for two-phase numerical schemes [5]. It consists of a 12 m vertical pipe initially filled with a mixture of air ($\alpha_a = 0.2$ and $\rho_a = 1$ kg.m^{-3}) and water ($\alpha_w = 0.8$ and $\rho_w = 1000$ kg.m^{-3}). The boundary condition at the top of the tube is a fixed 10 m.s^{-1} water inflow on the volume fraction of 0.8 with no air flux. The bottom of the tube is open to ambient pressure $P = 10^5$ Pa. With these conditions and under the action of gravity $g = 10$ m.s^{-2}, the water jet accelerates and stretches. In practice, the equations of state of water and air are approximated by stiffened and perfect gases respectively (1). In the limit of incompressible water, analytical solutions are known for the air volume fraction that allow the comparison of numerical results. The different features of this test are mostly on advection and amplification of a volume fraction discontinuity, with marginal compressibility effects. Figure 4 displays the volume fraction map and profile for the Ransom's water faucet problem performed on a dynamically and randomly distorted mesh. The numerical domain $\Omega = [0; 12] \times [0; 1.2]$ is initially meshed with a uniform coarse Cartesian grid composed by 100×10 cells. This mesh is then dynamically distorted to the skewed configuration by the grid velocity defined by $\boldsymbol{w} = (w_x, w_y)$ where w_x and w_y are random numbers between -10^{-2} and $+10^{-2}$. In Figure 4(b) all the points of the mesh are plotted for two mesh sizes $I = 120 \times 40$ and $I = 240 \times 80$.

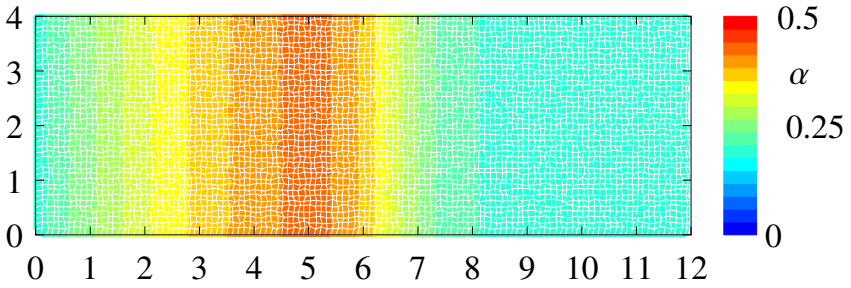

(a) Two-dimensional density map

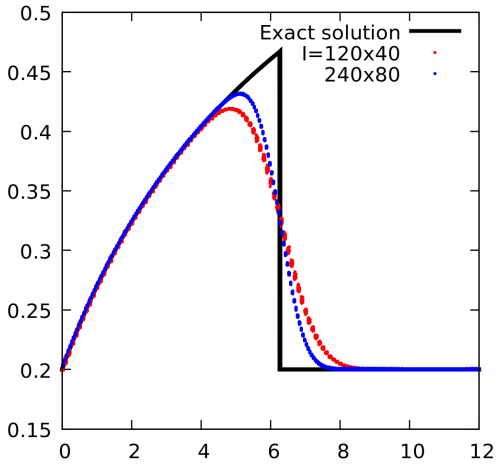

(b) One-dimensional superposition of all volume fraction points

FIGURE 4 – Volume fraction map and profile for the two-dimensional Ransom's water faucet problem on randomly and dynamically distorted grid. Computations are performed with CFL $= 0.8$. The ALE mesh on the volume fraction map (top) is $I = 120 \times 40$, every displayed macro cell (white lines corresponds to 1×1 numerical cells.

3.5 2D nine-phase crossing test

In this test, eight packets of heavy fluids $\rho_l = 1000$ cross in a surrounding light gas $\rho_g = 1$ at pressure $P = 10^5$. The gas is perfect with $\gamma = 1.4$ and the heavy fluids are stiffened gases with $\gamma = 7$. Initial domain is $\Omega = [-3;3] \times [-3;3]$ with $I = 480 \times 480$ cells. Initial volume fractions of the packets are identical Gaussian profiles of amplitude 0.15 and variance 0.2 in both dimensions. Packets' initial positions and velocities are (notice matched $\pm$ and $\mp$ signs)

$$\begin{array}{cccc} x & y & \mu_x & \mu_y \\ \pm 1 & 0 & \mp 1000 & 0 \\ 0 & \pm 1 & 0 & \mp 1000 \\ \pm 2 & 0 & \mp 2000 & 0 \\ 0 & \pm 2 & 0 & \mp 2000 \end{array} \tag{4}$$

In order to demonstrate the stability and robustness of multiGEECS, the computation are carried out on a shrink-then-stretch swirling grid with the corresponding grid velocity

$$w_x = 3\sin(\pi x)\cos(\pi y) - 1.5\eta x \ , \tag{5a}$$

$$w_y = -3\cos(\pi x)\sin(\pi y) - 1.5\eta y \ , \tag{5b}$$

where $\eta = 0.5$ for $t < 10^{-3}$ and $\eta = -0.5$ for $t > 10^{-3}$.

Figure 5 display the volume fraction profiles for the nine-phase crossing test on a shrink-then-stretch swirling grid. At time $t = 10^{-3}$, all the packets cross in the middle of the domain and the volume fraction of the gas drops to ≈ 0.04. At final time 2.10^{-3}, the packets are separated and only modified by numerical diffusion—as there is no particular exchange term between phases, they only interact via pressure forces. This test represents a starting point for the simulation of gas–particles flows in CEA applications involving sprays of heavy droplets into light gas.

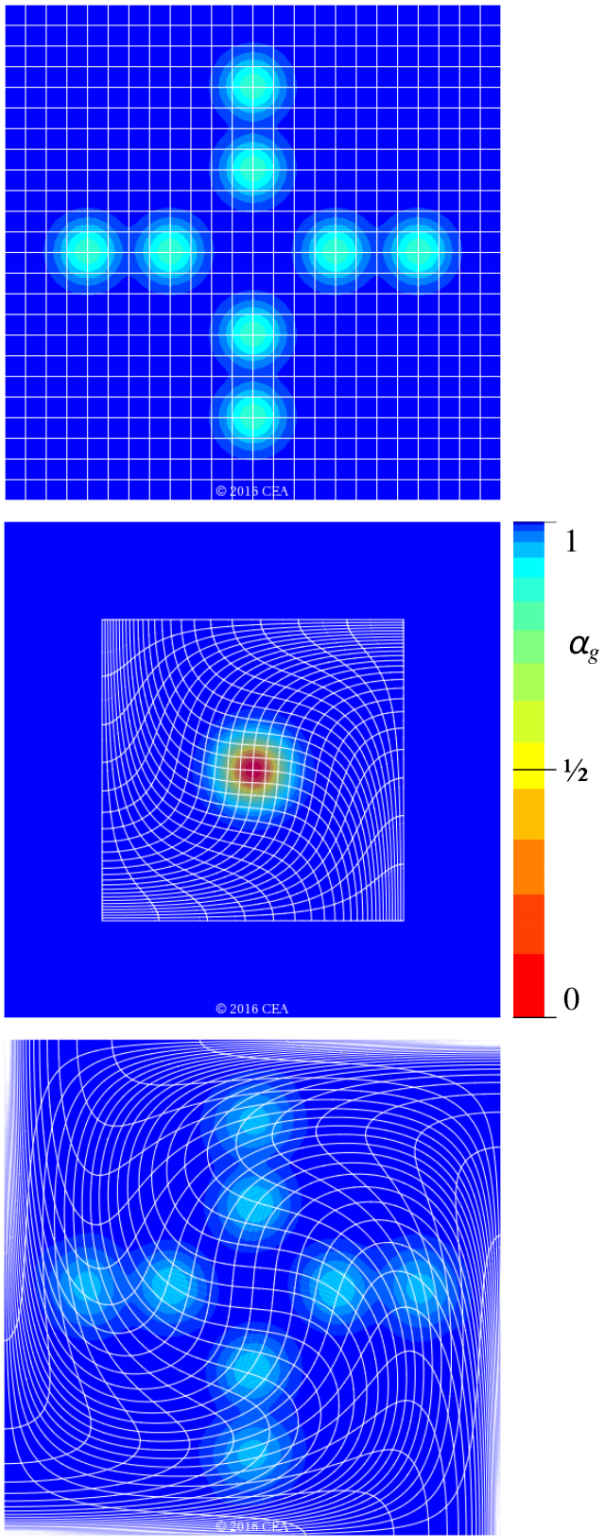

FIGURE 5 – Volume fraction maps at time $t = 0$ (top), $t = 10^{-3}$ (middle), and final time $t = 2.10^{-3}$ (bottom) for the nine-fluids crossing test on a shrink-then-stretch swirling grid. Computations are performed with CFL $= 0.7$ and $I = 480 \times 480$, every displayed macro cell (white lines) corresponds to 20×20 numerical cells.

Références

[1] Vazquez-Gonzalez, T., Llor, A., and Fochesato, C., Ransom test results from various two-fluid schemes : is enforcing hyperbolicity a thermodynamically consistent option ? *Int. J. Multiphase Flow*, 81 (2016), 104-112.

[2] Vazquez-Gonzalez, T., Llor, A., and Fochesato, C., A novel GEEC (Geometry, Energy, and Entropy Compatible) procedure applied to staggered direct-ALE scheme for hydrodynamics, *Eur. J. Mech. B Fluids* , submitted, 2016.

[3] Vazquez-Gonzalez, Schémas numériques mimétiques et conservatifs pour la simulation d'écoulements multiphasiques compressibles, PhD Thesis, Université Paris-Saclay, 2016.

[4] Arnold, G.S., Drew, D.A., and Lahey Jr, R.T., An assessment of multiphase flow models using the second law of thermodynamics, *Int. J. Multiphase Flow*, 16, p. 491, 1990.

[5] Ransom, V.H., Numerical benchmark test No2.1 : faucet flow, Multiphase Sci. Technol., 1 (1987), 465.

[6] Sedov, L. I., Similarity and dimensional methods in mechanics, Academic Press, 1959.

[7] Sod, G. A., A survey of several finite difference methods for system of nonlinear hyperbolic conservation laws, J. Comput. Phys., 27 (1978),1.

[8] Marchioli, C., and Soldati, A., Reynolds number scaling of particle preferential concentration in turbulent channel flow, *Proceedings of the 6th International Conference on Multiphase Flow*, Sommerfeld M. Ed., Martin-Luther Universitat, Halle-Wittenberg, Vol. 1, pp. 1-6, 2007.

[9] Batchelor, G.K., *An Introduction to Fluid Dynamics*, first ed., Cambridge Mathematical Library, Cambridge, 1967.